

Biassing and large-scale structure in a standard CDM N-body simulation

Andrei G. Doroshkevich^{1,3}, Richard Fong², and Olga Makarova³

¹ Theoretical Astrophysics Center, Juliane Maries Vej 30, DK-2100 Copenhagen Ø, Denmark

² Department of Physics, University of Durham, South Road, Durham DH1 3LE, England

³ Keldysh Institute of Applied Mathematics, Russian Academy of Science, Miusskaya Sq. 4, Moscow, 125047, Russia

Received 21 August 1996 / Accepted 25 July 1997

Abstract. We apply ‘core sampling’ analysis to a standard CDM N-body simulation, in which ‘galaxies’ are identified as high density peaks in the initial density field. The main concern of this paper is in the *general* insight the model provides into the possible relationship between dark matter (DM) and ‘galaxy’ large-scale structures at the present epoch.

The analysis finds the dark matter (DM) distribution to be dominated by a *hierarchical* distribution in richness of sheet-like structures, i.e. of Zel’dovich DM pancakes, over scales of $\sim 10\text{--}100 h^{-1}$ Mpc. On the other hand, the ‘galaxy’ large-scale structure is found to be bimodal, with the poorer structure dominated by filaments and the richer structure dominated by sheet-like elements.

The analysis also estimates a mean separation or characteristic scale for ‘galaxy’ filaments of $\approx 10.9 \pm 0.7 h^{-1}$ Mpc. With such a modest scale size we identify them as elements of ‘Large-Scale Structure’ or LSS. A natural interpretation of this difference in the ‘morphology’ of DM LSS from that of ‘galaxy’ LSS is that galaxy filaments may be expected to trace the high density ridges of DM Zel’dovich pancakes. The rich ‘galaxy’ sheet-like structures are found to have a mean separation of $\approx 75\text{--}80 h^{-1}$ Mpc. We call this ‘Superlarge-Scale Structure’ or SLSS. Also, as large a fraction as $\approx 60\%$ of the ‘galaxies’ are in SLSS. These are all in good agreement with the corresponding observational results.

However, this particular simulation was not found to possess the stable rich filamentary population seen in the observations. Nevertheless, the above results show that the form of the ‘galaxy’ spatial distribution has, on the whole, many similarities with that of the observed population, yet that of the DM distribution is distinctly different. The simulation thus provides an example of the profound effect biasing could have on the form of the observed large-scale structure in the Universe.

Key words: cosmology: theory – observations – large-scale structure of universe: formation and evolution: characteristic scales – N-body simulations: dark matter – general: galaxies

1. Introduction

The study of large-scale structure took on an entirely new perspective with the discoveries of filaments or chains of galaxies and rich sheet-like structures, such as galaxy superclusters and ‘great walls’, surrounding ‘great voids’ (see, e.g., Gregory & Thompson 1978, Kirshner et al. 1983, Oort 1983, de Lapparent et al. 1988, da Costa et al. 1988, Ramella et al. 1992, and, more recently, Shectman et al. 1996 and Ratcliffe et al. 1996). They provide vivid support for the picture predicted by the Zel’dovich approximation (Zel’dovich 1970) of an intricate random network structure of filamentary and sheet-like elements and, thus, for gravitational instability as the most natural physical mechanism for the formation of structure in the Universe. Numerous dynamical N-body simulations have since followed, showing, in particular, how generic such structure is for any gravitational instability model.

As a direct means of quantitatively studying filaments and sheets, Buryak et al. (1994, hereafter BDF) developed their ‘core sampling’ method of analysis. It measures the *mean free path* between structure elements along random core samples taken from the distribution. Besides being a measure familiar from many branches of physics for the description of a 3-dimensional distribution, the mean free path is especially apt for such very complex structure as here, providing a well-defined quantitative definition of the ‘mean separation’ of structure elements and, in the case of rich sheet-like structures, of the ‘mean size’ of ‘voids’. Furthermore, as developed by BDF, core sampling analysis is also able to discriminate *statistically* between filamentary and sheet-like structure elements, providing then estimates of their mean separations. These mean separations are, of course, *physical* characteristic scales of these structure elements.

Most recently, Doroshkevich et al. (1996, hereafter LCCSA) have applied the ‘core sampling’ analysis to great effect to the very large and deep Las Campanas Redshift Survey (Shectman et al. 1996, hereafter LCRS). As the mean separation of galaxy filaments is $\sim 10 h^{-1}$ Mpc, we follow BDF and call these elements of ‘Large-Scale Structure’ (LSS) and rich sheet-like structures, with mean separation $\sim 50\text{--}100 h^{-1}$ Mpc, elements

of ‘Superlarge-Scale Structure’ (SLSS). The ‘core sampling’ analysis of BDF, especially when applied to the LCRS, thus provides a basic means of quantifying this *bimodal* ‘morphological’ distribution of large-scale structures in the galaxy population.

But, interestingly, the same analysis applied to the DM distributions in N-body simulations finds that, on LSS scales, sheet-like elements dominate, in complete contrast to galaxies in which, in terms of their numbers, filaments dominate on LSS scales (Doroshkevich et al. 1997a, hereafter DFGMM). To understand how such a difference can arise, we need to investigate N-body simulations of the galaxy distribution. Thus, in this paper we investigate both the ‘galaxy’ and dark matter (DM) distributions in the same N-body simulation. The simulation is based on a well tried and tested N-body code and biasing mechanism for the standard cold dark matter (CDM) scenario, with ‘galaxies’ defined as the highest peaks in the initial density field, perhaps the simplest of possible ‘biasing’ algorithms (Bardeen et al. 1986, hereafter BBKS).

We have, furthermore, developed a theoretical description of the formation and evolution of large-scale structure in the universe by extending the Zel’dovich approximation to provide an approximate analytic expression for the mean separation of DM LSS elements, i.e. DM Zel’dovich pancakes, as a function of redshift and the power spectrum for the initial density inhomogeneities (DFGMM). Since it is thought that initially underdense regions (UDRs), equivalently regions of positive gravitational potential, expand faster than the rest of the universe to become the galaxy ‘voids’ we see today, a similar analytic solution can also be found for the mean separation of the SLSS ‘great walls’ observed in galaxy redshift surveys by applying the theory of random processes to the initial gravitational potential field (Buryak et al. 1992, Demiański & Doroshkevich 1992 and DFGMM). Thus, our ‘core sampling’ analysis also provides a test of the usefulness of this theoretical description.

We provide in Sect. 2 a brief resumé of the ‘core sampling’ method of analysis. The analysis of the ‘galaxy’ and DM structure in the simulated catalogues is presented in Sect. 3. We conclude with Sect. 4, in which the results of the analysis are discussed in the context of the formation and evolution of LSS and SLSS in the Universe.

2. ‘Core sampling’ analysis

The ‘core sampling’ method of analysis of large-scale structure in the Universe has been fully described in previous papers, particularly BDF, LCCSA and Doroshkevich et al. 1997b. Here, we simply briefly outline the method and point out some salient points and assumptions.

We are concerned in this paper with scales $\gtrsim 10 h^{-1}$ Mpc, for which the galaxy correlation function is close to zero. We, thus, expect that structure elements may well be approximately Poisson distributed along an arbitrary straight line. Thus, to study this distribution, we simply divide the N-body simulations into cylindrical core samples, our ‘arbitrary straight lines’. The core samples are then organised into an ‘equivalent single 1-dimensional field’ by ignoring the distance from the core sample

axis of an object, be it a DM particle or ‘galaxy’, and combining the separate resulting fields one after the other along a line, with the first object of the field placed on top of the last object of the preceding field. It is the objects’ positions along this equivalent single field to which we apply standard 1-dimensional cluster analysis.

It is well known (see, e.g., Buryak et al. 1991) that for a 1-dimensional Poisson-like sample the mean number of detected ‘clusters’ for a linking length, R_l , is given by the relation

$$N_l = N_0 \exp(-R_l/R_0), \quad (2.1)$$

where N_0 and R_0 are, respectively, the number of and the mean distance between the *underlying* Poisson distributed objects, i.e. the ‘true clusters’. At small linking lengths (\lesssim the cluster size) we would be exploring the inner structure of these ‘true clusters’, and the resulting values for N_l would depart from (2.1). The results of this and our other papers, BDF, LCCSA and DFGMM, not only show this departure from Poissonian for small linking lengths, they most importantly show also that the data points do follow well Eq. (2.1) for large enough linking length (see, in particular, Fig. 4 of LCCSA) and, thus, provide important *empirical* evidence that there exists conglomerations of points that are approximately Poisson distributed.

We have made direct tests of the method with simulations of the simplest model, that of random ‘galaxy’ filaments and sheets (BDF), and simulations based on Voronoi tessellation (Doroshkevich et al. 1997b). We also expect to find a close correspondence of our ‘measurements’ using this analysis with the predictions of the theory developed in DFGMM. Consequently, we naturally identify these conglomerations of points in the observational and N-body data as our elements of large-scale structure. In particular, we make the working assumption that the distribution of structure elements along a random straight line is approximately Poissonian.

A further and quite remarkable advantage of our core sampling analysis is that it can distinguish between filamentary and sheet-like behaviours. Let σ_f and σ_s be the *surface* density of filaments and the *linear* density of ‘sheets’, respectively. It is easy to show (BDF, LCCSA) that the mean number, N_0 , of *all* structure elements in a long narrow cylinder is given by

$$N_0/L = \sigma_s + \pi\sigma_f R_{core}, \quad (2.2a)$$

where L and R_{core} are the length and radius of the cylinder, and that

$$R_0^{-1} = \sigma_s + \pi\sigma_f R_{core} \quad (2.2b)$$

gives their mean separation, R_0 . Thus, by studying how the mean number of structure elements depends on R_{core} , Eq.s (2.2) allow us to obtain empirically the structure parameters, σ_f and σ_s , or equivalently the characteristic scales,

$$D_f = \frac{1}{\sqrt{\sigma_f}} \quad \text{and} \quad D_s = \frac{1}{\sigma_s}.$$

Obviously, both N_0/L and R_0^{-1} are identical for a Poisson sample and, with our working assumption, we expect

$$L/N_0 \approx R_0, \quad (2.3)$$

where L/N_0 and R_0 come from fitting the data points with the relationship (2.1) for large enough linking lengths (for an explicit example, see Fig. 4 of LCCSA). However, as gravity acts on all scales and as we have already pointed out, we only expect these equations to be approximately obeyed. Indeed, we can make use of the situation and treat Eqs. (2.2a) and (2.2b) independently, using the difference in the results as an estimate of the possible error in our estimates.

Finally, in order to study the dependence on richness and to provide a more complete characterization of structure, we also apply the analysis to catalogues obtained through the rejection of poorer clusters (see, e.g., LCCSA for a more detailed discussion). Here, this culling process is done through an initial use of the above 1-dimensional clustering analysis using a *fixed* linking length, R_{rej} , of $2 h^{-1}$ Mpc and rejecting all galaxies in clusters with multiplicity less than some threshold multiplicity, μ_{th} . Perhaps the most convenient choice of parameter for characterising the resulting subsample is the fraction of objects retained in the catalogue after culling rather than μ_{th} , using f_{gal} for the fraction of ‘galaxies’ retained and f_{DM} for the similar fraction of DM particles.

3. Analysis of an N-Body CDM simulation with ‘galaxies’

3.1. The data

Here we apply the ‘core sampling’ analysis to the resulting ‘galaxy’ and DM catalogues at $z = 0$ for one of the simulations that Eke et al. (1996) have performed using the tried and tested N-body code and biasing algorithm introduced by White et al. (1987) for generating mock galaxy catalogues. They are based on a standard CDM initial power spectrum (BBKS) in the usual cubic computational box with side $256 h^{-1}$ Mpc. The number of DM particles is 128^3 , giving a resolution of about $2 h^{-1}$ Mpc. They are evolved to have a bias factor for ‘galaxies’ of $b = 1.58$ and, thus, a $\sigma_8 = 0.63$ for the dark matter distribution at the present epoch, $z = 0$. Using the resampling technique of statistics, ‘galaxies’ were randomly selected from the set of DM particles using the probability distribution given by the high peaks bias prescription of BBKS. The $1.1 \cdot 10^5$ ‘galaxies’ thus selected was dictated by the constraints of available disk space and computer time and provides for a reasonable ‘galaxy’ density of $\sim 0.01 h^3 \text{ Mpc}^{-3}$. Ratcliffe (1996) and Ratcliffe et al. (1996) have confirmed that these simulations give the correct galaxy two-point autocorrelation function over scales of $\lesssim 10 h^{-1}$ Mpc, where it has been well determined observationally, in a comparison with the results for the recent Durham/UKST Redshift Survey.

For applying the core sampling analysis, $3 \times 25 \times 25$ separate cylinders with a radius $a_{cyl} = 2.5 h^{-1}$ Mpc and oriented along the 3 coordinate axes were prepared. As the distance between neighbouring cylinders is $2 a_{cyl}$, larger than the correlation length for the DM particles, $r_0^{DM} \approx 4 h^{-1}$ Mpc, the correlation between objects in different cylinders is negligible. The core samples thus constructed contained $\approx 9 \times 10^5$ DM particles and $\approx 6.4 \times 10^4$ ‘galaxies’.

The global number density of DM particles and ‘galaxies’ are then

$$\begin{aligned} \langle \rho_{DM} \rangle &\approx 0.125 h^3 \text{ Mpc}^{-3}, \\ \langle \rho_{gal} \rangle &\approx 0.4 \times 10^{-2} h^3 \text{ Mpc}^{-3} \end{aligned}$$

and the corresponding mean *linear* densities in the core samples are

$$\langle \rho_{DM}^{cyl} \rangle \approx 1.9 h \text{ Mpc}^{-1}, \quad \langle \rho_{gal}^{cyl} \rangle \approx 0.13 h \text{ Mpc}^{-1}$$

The latter value is similar to the linear densities of galaxies in the core samples used in the similar analysis of the Las Campanas Redshift Survey (LCCSA).

Finally, we write down the expected theoretical values, using the analytical expressions of DFGMM, for the structure parameters for this simulation, i.e. for the BBKS CDM spectrum with $h = 0.5$, $k_{min} = 1.2 \cdot 10^{-2} h^{-1} \text{ Mpc}$ and $k_{max} = 3.1 h^{-1} \text{ Mpc}$:

$$\begin{aligned} D_{SLSS}^{theor} &= 87 h^{-1} \text{ Mpc}, \quad D_{LSS}^{theor}(z=0) = 6.2 h^{-1} \text{ Mpc}, \\ v_{rms} &= 710 \text{ km/s}. \end{aligned} \quad (3.1)$$

3.2. The results for the ‘galaxy’ distribution

In general, the core sampling results for the spatial structure of the ‘galaxy’ distribution in this simulated catalogue are similar to those for real galaxies (BDF, LCCSA). Fig. 1 shows that for the full sample, $f_{gal} = 1$, filamentary structure dominates. Sheet-like structures only appear for $f_{gal} \lesssim 0.7$, i.e. when the catalogue is restricted to richer elements using the culling technique mentioned in Sect. 2. Fig. 1 also shows that these ‘sheets’ have a characteristic scale, $D_s^{gal} \approx 75\text{--}80 h^{-1} \text{ Mpc}$. Unfortunately, the computational box is only about three times larger, and we should perhaps not expect to obtain a very representative estimate of the mean separation of SLSS elements for this model. Bearing this in mind, the result is in reasonable agreement with the theoretical estimate of Eq. (3.1), supporting DFGMM’s proposal for a quantitative theoretical description of the formation and evolution of large-scale structure in the universe. However, this result for D_s^{gal} is in surprisingly good agreement with our best observational results so far, since the similar analysis of the LCRS gives an estimate of $77 \pm 9 h^{-1} \text{ Mpc}$ (LCCSA). But, realistically, we should note the large error in our estimate for D_s^{gal} and recall that our principal purpose in this paper is simply to investigate with this one simulation the possible general relationship between DM and ‘galaxy’ large-scale structures at the present epoch. Fig. 2 shows, for comparison, the observational results for $D_s(f)$ and $\sigma_f(f)$ for a sample of the LCRS.

The measurements for LSS were found for the culling parameter in the range $0.6 \leq f_{gal} \leq 1$. From the values at $f_{gal} \approx 1$, we estimate a surface density of filaments for the full sample of

$$\sigma_f^{gal} \approx (0.84 \pm 0.1) \times 10^{-2} h^2 \text{ Mpc}^{-2},$$

corresponding to a mean separation of filaments of

$$D_f^{gal} = \sigma_f^{-1/2} \approx 10.9 \pm 0.7 h^{-1} \text{ Mpc}.$$

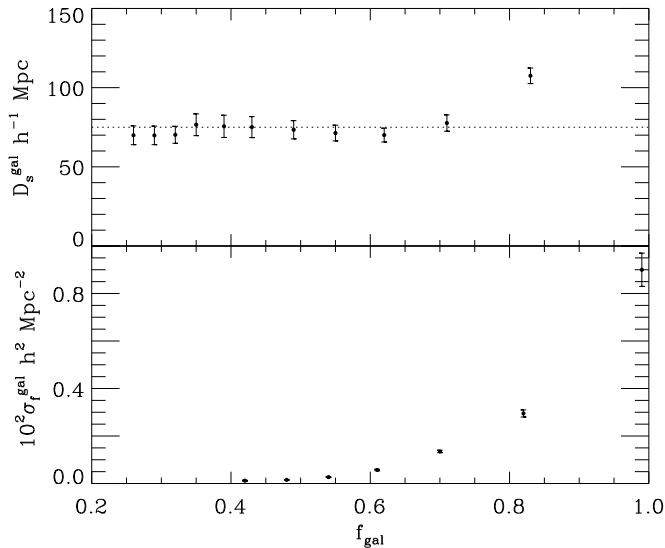


Fig. 1. Results for the simulated ‘galaxy’ distribution: (a) the mean separation, D_s^{gal} , of sheet-like elements and (b) the mean surface density, σ_f^{gal} , of the filamentary component. Both are determined in comoving space and plotted vs. f_{gal} , the fraction of ‘galaxies’ left after the culling of poorer clusters (see Sect. 2).

This is in good agreement with the LCCSA observational results,

$$D_f^{LCCSA} \approx 12.9 \pm 0.3 h^{-1} \text{ Mpc},$$

but these values are a factor of 2 greater than the expected theoretical value, Eq. (3.1). We shall see in the next section that in the simulation this is as a result of the biasing between ‘galaxies’ and DM. Since $D_s^{gal} \approx 7 \times D_f^{gal}$, there are many fewer SLSS structure elements and, in terms of their numbers, filaments dominate the structure.

However, the rapid decrease of σ_f^{gal} with the rejection of ‘galaxies’ through the culling process implies that ‘galaxies’ are strongly concentrated in SLSS, i.e. in ‘walls’ and richer clumps. More exactly, Fig. 1 shows very clearly that $\approx 60\%$ of the ‘galaxies’ cannot be identified with LSS filaments and belong instead to SLSS, despite the dominance in numbers of the filamentary structure. This result is also in good agreement with the LCRS results (LCCSA). But, Fig. 2b also shows a stable sub-population of richer filaments for the LCRS, i.e. $\sigma_f^{LCRS} \approx \text{const.}$ for $f_{gal} \lesssim 0.8$, and such a population is absent in the simulation.

As the spatial structure is distorted in galaxy redshift surveys by their peculiar motion, simulations also provide a very important test. The most well known distortion is, of course, that due to the ‘Fingers of God’ effect, which occurs for rich clumps of galaxies. In standard CDM simulations, such as the one we are analysing here, the peculiar velocities of ‘galaxies’ in a rich clump is $\sim 700 \text{ km s}^{-1}$, significantly greater than the observed peculiar velocity of $\sim 300\text{--}400 \text{ km s}^{-1}$ and giving a sizeable ‘Fingers of God’ effect. To test this effect on the LSS parameters they were estimated in two ways: firstly, using the comoving coordinates of the ‘galaxies’ and, secondly, using the redshift coordinates along the cylinder axis. We found that for LSS the difference amounts to no more than 10%, about the

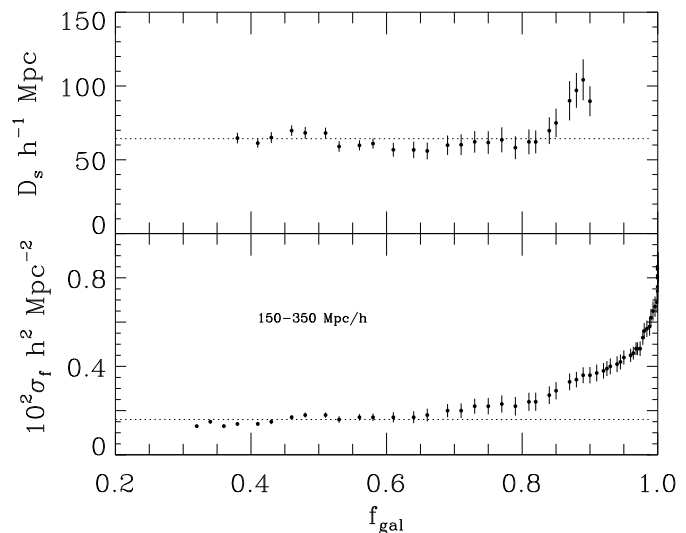


Fig. 2. Example of the results of the ‘core sampling’ analysis of the Las Campanas Redshift Survey galaxy catalogue: (a) the mean separation, D_s , of sheet-like elements and (b) the mean surface density, σ_f , of the filamentary component. See LCCSA for the complete analysis. As with Fig. 1, f_{gal} is the fraction of galaxies left after culling.

same as the the measurement errors themselves. Thus, as far as the LSS measures are concerned, the systematic effect caused by peculiar velocities is small and they do not blur out the LSS elements so much as to make them undetectable in redshift space, the space we generally have to use for the observations. As to SLSS, the structure elements are so rich and the scale so large as to be essentially unaffected by such redshift space distortions.

3.3. Analysis of the DM particle distribution

Fig. 3 presents the main results of the analysis. It can be seen from Fig. 3b that with the threshold, $\mu_{th} = 2$, when $f_{DM} \approx 0.9$, the mean surface density of filaments begins to vary extremely rapidly with the culling parameter, f_{DM} , with the separation between ‘filaments’ becoming similar to the mean separation of $1 - f_{DM} \approx 0.1$ of DM particles. Thus, $\approx 10\%$ of DM particles may be considered as a more or less realistic estimate of a quasi-homogeneous background of the DM particles which are not yet integrated into structure elements. In the ‘core sampling’ analysis they appear as poorly populated artificial structure elements. This effect is absent for galaxies; we expect that DM structure elements need to be well developed for galaxy formation to occur and that, consequently, all galaxies are in either clearly formed LSS or SLSS structure elements. Consequently, we shall only consider the more well defined results from culled DM particle catalogues using a threshold, $\mu_{th} \geq 2$.

The analysis clearly detects LSS in the spatial distribution of DM particles. Not only is this structure composed of filaments, but even at a scale of $\sim 10 h^{-1} \text{ Mpc}$, it is also composed of sheets, which contrasts markedly with the bimodal galaxy distribution, in which the sheet-like structure belongs strictly to SLSS and not to LSS. Thus, although the surface density of the DM filaments for the ‘full sample’ is similar to that in the

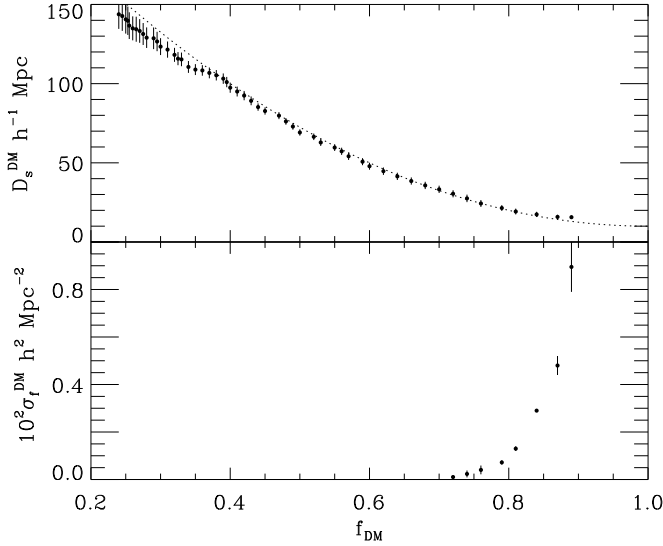


Fig. 3. For the DM distribution, (a) the mean separation, D_s^{DM} , of sheet-like elements and (b) the mean surface density, σ_f^{DM} , of the filamentary component, again as calculated in the comoving space and plotted vs. the fraction of matter, f_{DM} , left after culling. The dotted line represents the fit of Eq. (3.3).

‘galaxy’ population,

$$\sigma_f^{DM} \approx 0.9 \cdot 10^{-2} h^2 \text{ Mpc}^{-2},$$

it decreases rapidly with f_{DM} . The relationship,

$$\sigma_f^{DM} \approx 0.04 \left[1 + 2.5 \exp\left(\frac{1 - f_{DM}}{0.04}\right) \right]^{-1} h^2 \text{ Mpc}^{-2}, \quad (3.3)$$

provides an approximate fit of these σ_f^{DM} results. Indeed, Fig. 3 shows that this population includes no more than 20% of DM particles, because of this rapid decrease with f_{DM} . In turn, this implies that they are placed preferentially in UDRs. This is expected theoretically and they correspond to a population of structure elements that form later at a low rate. Even later, they will accumulate more matter, transforming into recognizable pancakes, i.e. sheet-like structures.

The sheet population, with the characteristic scale $D_s^{DM} \approx 16 h^{-1} \text{ Mpc}$, and containing some 80% of the DM particles, dominates in the DM distribution. This is in contrast to the ‘galaxy’ distribution, which, in terms of their numbers, is dominated by filamentary structure (Sect. 3.2).

The characteristic scale of the DM sheet distribution increases with threshold and it can be written vs f_{DM} as

$$D_s^{DM} = 1/\sigma_s^{DM} \approx 10 \left[1 + \left(\frac{1 - f_{DM}}{0.2}\right)^2 \right] h^{-1} \text{ Mpc}. \quad (3.4)$$

This expression fits the numerical data with an error of no more than 5-7% (Fig. 3).

For such a mixed population of filamentary and sheet-like structures for DM LSS, a common ‘characteristic scale’ needs

to be specially defined. A convenient measure for a mixed population is the diameter of spheres containing on average two LSS structure elements:

$$D_{f-s} = 2 \left(\sigma_s + \sqrt{\sigma_s^2 + \pi \sigma_f} \right)^{-1}. \quad (3.5)$$

Thus, the measured, i.e. the ‘core sampling’ estimated, characteristic scale of *dark matter* LSS is for the ‘full sample’, i.e. for $f_{DM} = 1$,

$$D_{f-s}^{DM} \approx (8 \pm 1.2) h^{-1} \text{ Mpc}.$$

The good agreement with the expected theoretical estimate of $\approx 6.2 h^{-1} \text{ Mpc}$, Eq. (3.1), bodes well for the analytic description proposed by DFGMM for the evolution and formation of large-scale structure in the universe. It is clear now that the factor of 2 larger value for D_f^{gal} in the previous section is due to the biasing between ‘galaxies’ and DM, rather than any serious discrepancy with the theory developed by DFGMM.

Also unlike the ‘galaxy’ distribution, the mean separation of DM structure elements is a continuous monotonically increasing function of richness. In other words, DM structure elements seem to be *hierarchically* distributed, making it impossible to pick out an SLSS scale for the very rich structure elements. Nevertheless, it is significant that more than 50% of DM particles are concentrated in structure elements with characteristic separations $> 60 h^{-1} \text{ Mpc}$, as the ‘galaxy’ elements with such large separations also contain more than 50% of the ‘galaxies’. Therefore, even though there are so few SLSS elements in the simulation, SLSS is clearly as important a component as LSS in the ‘large-scale structure of the universe’. We discuss this further in the next section.

3.4. The relationship between ‘galaxies’ and DM; the bias on LSS and SLSS scales

The domination of sheet-like structures in the DM distribution supports the main conclusion of Zel’dovich’s theory of structure formation through gravitational instability (Zel’dovich 1970), which predicted the formation of 2-dimensional ‘pancakes’ as the most typical elements of large-scale structure in the universe. Observationally, we have quite the reverse situation, as there filaments dominate in the galaxy distribution, forming a ‘random network structure’ in the Universe. As this is also true for the ‘galaxies’ in the simulation, it seems that this ‘morphological’ domination by filamentary structure in the observational data is more an embodiment of the ‘biasing’ process discussed by, e.g., BBKS, than a direct consequence of gravitational instability.

It is natural to attempt to draw the inference that galaxies are simply tracing the high density ridges of DM Zel’dovich pancakes and that these results suggest that significant DM halos surround galaxy filaments. Unfortunately, ‘core sampling’ does not identify individual filaments and sheets, but simply finds *statistically* the underlying filamentary and sheet-like populations (Sect. 2). However, some idea of the relationship between ‘galaxies’ and DM can be obtained by comparing, for a given culling criterion, μ_{thr} , the fractions f_{DM} and f_{gal} . Then, if ‘galaxies’ trace the high density DM clumps, we would expect

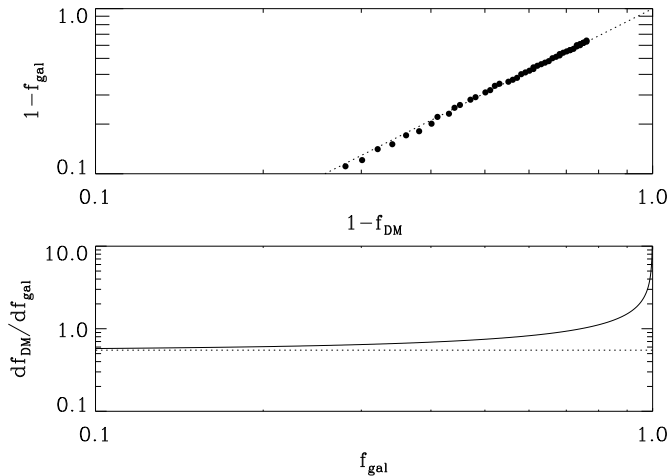


Fig. 4. Top panel: The fraction of galaxies, f_{gal} , vs. fraction of DM, f_{DM} , remaining in the sample after the rejection of both DM particles and galaxies using the same rejection parameters (i.e. linking length and threshold richness). Bottom panel: Bias in the galaxy-DM distribution (df_{DM}/df_{gal}) vs. the fraction of galaxies left after culling.

these two fractions to change proportionally at high enough thresholds. Thus, with different μ_{thr} , f_{gal} can be found as a function of $(1 - f_{DM})$. This and df_{DM}/df_{gal} are presented in Fig. 4 and can be fitted by the simple relations

$$f_{gal} = 1 - (1 - f_{DM})^{1.8}, \quad (3.6)$$

$$df_{DM}/df_{gal} = 0.55 (1 - f_{gal})^{-0.44}. \quad (3.7)$$

These expressions show that, for massive elements with $f_{DM} \ll 1$, f_{gal} is, indeed, $\propto f_{DM}$. However, for $f_{gal} \rightarrow 1$ a strong bias is seen to be present, a result that is perhaps more interesting considering its physical implications.

A more detailed examination of Fig. 4 shows that, as expected, at low thresholds the 10-15% of quasi-homogeneously distributed DM particles are quickly culled with little loss of ‘galaxies’. The relationship at higher thresholds suggest a low relative fraction of ‘galaxies’ to DM for the weaker DM pancakes in UDRs, with quite possibly some of these DM pancakes having no ‘galaxies’ at all. With higher thresholds, these fractions correspond clearly to rich SLSS structure elements, with more than 50% of ‘galaxies’ and DM in structure elements whose mean separations are $> 60 h^{-1}$ Mpc. Here, the relative fraction of ‘galaxies’ to DM is high and relatively stable, but the essential difference in their SLSS properties can be clearly seen from Figs. 1 and 3. Fig. 1 shows a bimodal distribution for the ‘galaxies’ with a ‘stable’ SLSS population, i.e. with a well-defined SLSS characteristic scale for $f_{gal} \lesssim 0.7$, whereas Fig. 3 shows a hierarchical sheet-like distribution dominating the DM distribution.

These differences are, of course, produced by the procedure of ‘galaxy’ choice, which in this simulation followed the BBKS prescription, and Bower et al. (1993) have shown that such a prescription for the bias does lead to a strong difference in the correlation properties of the two populations. Possible physical sources for such a bias have been discussed by Buryak et

al. (1992), DFGMM and Demiański & Doroshkevich (1997), who point out two well-known effects likely to give rise to bias. They are the gravitational potential (see Sect. 1) and the possible reheating of the baryonic component by the X-ray and UV radiation from the first objects that were formed. Such a reheating of the baryonic component could well inhibit the formation of galaxies in weak DM pancakes in UDRs (White & Rees 1978, Shapiro, Giroux & Babul 1994, Fong, Doroshkevich & Turchaninov 1995), and the definition in the simulation here of a ‘galaxy’ as a high density peak imitates well the possible influence of reheating. Such weak DM pancakes would correspond to the ‘phantoms’ or ‘hot pancakes’ of Doroshkevich (1983). We might hope to detect ‘phantoms’ as absorption lines in the spectra of quasars that are not associated with any galaxy. The simulations of Hernquist et al. (1996) would strongly support such an explanation.

It is especially significant that such lines were observed in the central area of a large void in the UV spectrum of the quasar, 3C 273 (Morris et al. 1993). Three weak lines, with separations between them of $7.5 h^{-1}$ Mpc and $9.3 h^{-1}$ Mpc, are located at least $5 h^{-1}$ Mpc from the nearest faint galaxy. Thus, there is reason to consider this as the first observational evidence for DM walls, a hitherto unknown constituent of the large-scale structure of the universe. Interestingly, Stocke et al. (1995) and Shull et al. (1996) have found new examples of such lines, and we might hope that this is the start of an active research programme to obtain many more examples, to provide soon a first statistical study of observed ‘phantoms’, i.e. DM walls, inside well established galaxy ‘voids’.

4. Conclusions

The ‘core sampling’ analysis of an N-body simulation, with the particles in the highest peaks in the initial density field identified as ‘galaxies’, has provided us with an insight into the possible relationship between galaxies and matter in the Universe. Whether expected or not, the biasing mechanism here has clearly produced a ‘galaxy’ distribution quite unlike the underlying DM distribution. Besides the quasi-homogeneous background of $\sim 10\%$ of the DM particles, the DM population in this simulation is dominated by a *hierarchical* distribution in richness of sheet-like structures on scales of ~ 10 - $100 h^{-1}$ Mpc, whereas that of ‘galaxies’ is somewhat similar to the observations, consisting of a *bimodal* distribution of filaments and sheets with distinctly different characteristic scales, with ‘galaxy’ filaments as poorer structure elements and sheets richer ones. Further, like the observations (LCCSA), about 40% of the ‘galaxies’ are in filaments with mean separation $\approx 10.9 \pm 0.7 h^{-1}$ Mpc, in good agreement with the observed scale of $12.9 \pm 0.3 h^{-1}$ Mpc, with the remaining $\approx 60\%$ in stable rich sheet-like structures with mean separation ≈ 75 - $80 h^{-1}$ Mpc, also in agreement with the observed $77 \pm 9 h^{-1}$ Mpc. However, unlike the observations, these ‘galaxy’ filaments seem to follow a hierarchical distribution over the full range of measurable scales and the observed stable population of rich filaments with a characteristic scale of $\approx 30 h^{-1}$ Mpc is not seen in this particular simulation. Nev-

ertheless, the many similarities we find with the observations show again how successful the standard CDM model is in providing an approximate description of large-scale structure in the universe.

On the scale of LSS, the discussion of Sect. 3.4 showed that the ‘core sampling’ results are consistent with the natural perception that ‘galaxy’ filaments are embedded in DM sheets. In other words, ‘galaxy’ filaments trace the high density ridges of DM Zel’dovich pancakes, which in their turn constitute anisotropic halos around ‘galaxy’ filaments. Clearly, such a strong connection between the DM LSS structure elements and those of the ‘galaxy’ distribution is to be expected here, as ‘galaxies’ were defined as maxima of the density distribution and the density and velocity fields are strongly related in the standard CDM cosmogony. However, as filamentary structure also dominates the observed galaxy distribution (LCCSA), this relationship between DM Zel’dovich pancakes and galaxy filaments is most probably quite a general one. There will also be quite weak DM LSS sheets without galaxies in UDRs and, thus, in galaxy ‘voids’, and these could be the explanation for the observation of $Ly-\alpha$ absorption clouds in ‘voids’, as discussed in Sect. 3.4. Indeed, the interpretation for the distribution of the $Ly-\alpha$ lines seen in the absorption spectra of QSOs as being simply due to a hot gas component around such DM LSS structure elements is now being pursued with keen interest (Miralda-Escudé et al. 1996, Petitjean et al. 1995, Mückel et al. 1996, Hernquist et al. 1996).

In conclusion, our ‘core sampling’ analysis here and correlation function analysis (Ratcliffe 1996, Ratcliffe et al. 1996) show that the ‘galaxy’ spatial distribution has, on the whole, many similarities with that of the observed population. But, most interestingly, the ‘core sampling’ results, not only of this simulation, but also of simulations based on quite different initial power spectra (DFGMM), further show that the underlying DM distributions in these simulations possesses a fundamentally different structure from that of both the simulated and observed galaxy distributions at the present epoch. Although the biasing used in this simulation is somewhat hypothetical, being an *ansatz* for a practical algorithm, it probably mimics quite well a physical process such as the possible influence of secondary reheating in inhibiting galaxy formation in ‘voids’. The simulation thus provides an example of the profound effect biasing could have on the form of the observed large-scale structure in the Universe.

However, our analysis also shows differences with the observations. Besides the usual need to tune models so that measures, such as the correlation function, accurately match with the observed measures, there is, in particular, a lack in the simulation of a stable population of rich ‘galaxy’ filaments at a scale of $\approx 30 h^{-1}$ Mpc, as was found in the observations (LCCSA). It will be interesting to see if other future simulations of the galaxy distribution are able to exhibit such a population of rich filaments. Finally, we note how this simulation has also provided a demonstration of the usefulness of BDF’s core sampling analysis for exploring the fundamental nature of large-scale structure, revealing as it has the difference between the form of the struc-

ture in the DM distribution from that in the ‘galaxies’ of the simulation, as well as the difference just mentioned between the simulated and the observed galaxy distributions.

Acknowledgements. We would like to thank Shaun Cole for supplying the CDM simulation and Shaun Cole, Vincent Eke and Andrew Ratcliffe for useful discussions concerning the simulation. We would also like to thank the referee for useful comments helping to further clarify the paper. This work was supported in part by Denmark’s Grundforskningsfond through its support for an establishment of Theoretical Astrophysics Center. AGD is pleased to acknowledge INTAS for support for travel in connection with this work. AGD and OVM would also like to acknowledge support from the Center of Cosmo-Particle Physics, Moscow.

References

- Bardeen J.M., Bond J.R., Kaiser N., Szalay A., 1986, ApJ 304, 15
 Bower R.G., Coles P., Frenk C.S., White S.D.M., 1993, ApJ 405, 403.
 Buryak O.E., Demiański M., Doroshkevich A.G., 1991, ApJ 383, 41
 Buryak O.E., Demiański M., Doroshkevich A.G., 1992, ApJ 393, 464
 Buryak O.E., Doroshkevich A.G., Fong R., 1994, ApJ 434, 24 (BDF)
 da Costa L.N., Pellegrini P.S., Sargent W.L.W. et al., 1988, ApJ 327, 544
 de Lapparent V., Geller M.J., Huchra J.P., 1988, ApJ 332, 44
 Demiański M., Doroshkevich A., 1992, Int.J.Mod.Phys. D1 303
 Demiański M., Doroshkevich A., 1997, ApJ submitted.
 Doroshkevich A.G., 1983, Astron.Zh. Pisma 9, 188.
 Doroshkevich A.G., Tucker D.L., Oemler A.A. et al. 1996, MNRAS 283, 1281.
 Doroshkevich A.G., Fong R., Gottlöber S., Mückel J.P., Müller V., 1997a, MNRAS 284, 633 (DFGMM)
 Doroshkevich A.G., Gottlöber S., Madsen S., 1997b, A&AS 123, 495.
 Eke V.R., Cole S., Frenk C.S., Navarro J.F., 1996, MNRAS 281, 703.
 Fong R., Doroshkevich A.G., Turchaninov V.I., 1995, in Holt S.S., Bennet C.L., eds, Proc. 5th Maryland Astrophysics Conf., Dark Matter, AIP, New York, p. 429.
 Gregory S.A., Thompson L.A., 1978, ApJ 222, 784
 Hernquist L., Katz N., Weinberg D.H., Miralda-Escudé J., 1996, ApJ 457, L51.
 Kirshner R.P., Oemler A.J., Schechter P.L., Shectman S.A., 1983, AJ 88, 1285
 Miralda-Escudé J., Cen R., Ostriker J.P., Rauch M., 1996, ApJ 471, 582.
 Morris S.L., Weymann R.J., Dressler A. et al., 1993, ApJ 419, 524
 Mückel J.P., Petitjean P., Kates R., Riediger R., 1996, A&A 308, 17
 Oort J.H., 1983, ARA&A 21, 373
 Petitjean P., Mückel J.P., Kates R., 1995, A&A 295, L9
 Ramella M., Geller M.J., Huchra J.P., 1992, ApJ 384, 396
 Ratcliffe A., 1996, PhD thesis, Univ. of Durham
 Ratcliffe A., Shanks T., Broadbent A. et al., 1996, MNRAS 281, L47.
 Shapiro P.R., Giroux M.L., Babul A., 1994, ApJ 427, 25
 Shectman S.A., Landy S.D., Oemler A. et al., 1996, ApJ 470, 172.
 Shull J.M., Stocke J.T., Penton S.V., 1996, AJ 111 72.
 Stocke J.T., Shull J.M., Penton S.V. et al., 1995, ApJ 451 24.
 White S.D.M., Rees M.J., 1978, MNRAS 183, 341
 White, S.D.M., Frenk, C.S., Efstathiou, G., Davis, M., 1987, ApJ 313, 505.
 Zel’dovich Ya.B., 1970, A&A 5, 20

This article was processed by the author using Springer-Verlag L^AT_EX A&A style file L-AA version 3.